Available online at www.sciencedirect.com
ScienceDirect
Current Opinion in Chemical Biology

# Exploring RNA folding one molecule at a time

Elvin A Alemán, Rajan Lamichhane and David Rueda

RNA molecules fold into stable native structures to perform their biological function. RNA folding can be influenced by ions, co-factors, and proteins through numerous mechanisms. Understanding these mechanisms at the molecular level is important for elucidating the structure–function relationship in biologically important RNAs. Recent developments in single molecule spectroscopy have provided new approaches to investigate RNA folding and have allowed identification of kinetic intermediates that would otherwise remain hidden in ensemble-averaged experiments. Here we summarize some of these developments, which provide new insight into the effect of $Mg^{2+}$ ions in RNA folding landscapes, the role of cooperativity in RNA tertiary folding, the stepwise folding of RNA during transcription, and the hierarchical assembly of RNA–protein complexes.

**Addresses**
Department of Chemistry, Wayne State University, 5101 Cass Avenue, Detroit, Michigan 48202, USA

Corresponding author: Rueda, David (rueda@chem.wayne.edu)

**Current Opinion in Chemical Biology** 2008, **12**:647–654

This review comes from a themed issue on
Biopolymers
Edited by Philip Bevilacqua and Rick Russell

Available online 7th October 2008

1367-5931/$ – see front matter


**DOI** 10.1016/j.cbpa.2008.09.010

## Introduction

RNA has a unique ability to carry both genetic information and catalytic function. It plays key roles in the maintenance, transfer, and processing of genetic information and the control of gene expression [1–3]. According to the RNA World hypothesis, RNAs may have initiated life on Earth [4]. Naturally occurring functional RNAs find important applications in medicine, nanotechnology, and chemistry [5–9].

The RNA folding problem consists of understanding how linked nucleotides form a secondary and, subsequently, a functional tertiary structure. This reaction lies at the core of the structure–function relationship in RNA. To understand this relationship, it is essential to identify the fundamental principles of RNA folding (Figure 1), which translates into mapping the folding potential energy surface by determining the relative stability of all the intermediates involved and their activation energies. The stability of intermediate and native structures can be influenced by the interaction with metal ions, ligands, and proteins.

Single molecule spectroscopy (SMS) provides new insight into RNA folding. SMS has been used to elucidate the folding dynamics of small and large catalytic RNAs, the mechanism of tRNA accommodation into the ribosome, and to reveal heterogeneous folding dynamics in numerous RNAs [10••,11••,12,13••,14•,15,16••]. SMS shows that very few molecules in the macroscopic ensemble behave as its average; thus, interpreting the smooth, continuous changes characteristic of macroscopic observables in terms of smooth transformations at the molecular level can be misleading and incorrect [17]. SMS uncovers key structural, dynamic, and functional information otherwise hidden in the ensemble-averaged bulk experiment [18]. Perhaps the most astonishing discovery is that single molecules exhibit unexpected molecular memory effects in folding and catalysis, where a molecule rarely switches between different folded conformations [10••,13••,19•]. A likely explanation for this observation is that RNA folding landscapes are usually rough and contain kinetic traps that form isolated intermediates [20–22,23•]. Here, we summarize some of the latest developments in RNA folding using SMS [24•,25,26].

## Single molecule $Mg^{2+}$ jumps map RNA folding landscapes

As the backbone of RNA molecules is negatively charged, RNA folding is governed by metal ion condensation [20]. Monovalents promote secondary structure formation, and divalents help it collapse into a compact conformation [23•,27]. This key step involves the specific folding of helical junctions and single stranded internal loop lacking secondary structure. Recently, Scherer's group has reported a new single molecule approach that uses periodic [$Mg^{2+}$] jumps to study early events in RNA folding [28•]. The conformational dynamics of the fluorophore labeled catalytic domain of the large thermophilic RNase P RNA were monitored by single molecule Fluorescence Resonance Energy Transfer (smFRET, Figure 2a).

RNase P is an endonuclease involved in the maturation of tRNAs [29,30]. P RNA unfolds below 0.01 mM $Mg^{2+}$, and refolds above 0.1 mM $Mg^{2+}$. Successive jumps above and below these concentrations were used to observe (un)folding monitoring changes in FRET efficiency ($E_{FRET}$). Figure 2b shows two single molecule $E_{FRET}$ trajectories with the corresponding $Mg^{2+}$ jumps. Two types of conformational changes were observed: (i)

**Figure 1**

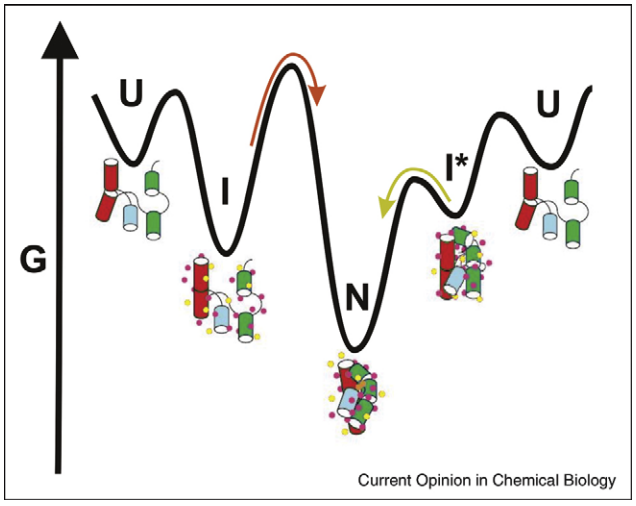


General representation of the free energy landscape of a RNA metal ion-induced folding where two possible folding pathways toward the native folded structure (N) are shown. In the case where a less collapsed intermediate is formed from the unfolded state (U → I), higher activation energy will correspond to the slower folding pathway (I → N). However, the faster folding pathway (I* → N) will match the formation of an intermediate structure (I*) that is more similar to the final native structure.

discrete transitions characteristic of barrier-crossing events at constant [$Mg^{2+}$] and (ii) a general electrostatic response (collapse or expansion) with exponential kinetics immediately following the jump (insets). Jumps from 0.01 to 0.1 mM [$Mg^{2+}$] exhibit only two FRET states at each concentration (I and IV, Figure 2c), whereas jumps from 0.01 to 0.4 mM and 1.0 mM [$Mg^{2+}$] exhibit four (I, II, III and IV, Figure 2c). Their analysis showed that P RNA folding from a high FRET state remains preferentially in the high FRET state, while folding from a low FRET state transitions to all four states (Figure 2c), indicating the presence of a memory effect of folding. Successive $Mg^{2+}$ jumps enable building pre-equilibrium cumulative histograms for folding (Figure 2c1 and c3) and unfolding cycles (Figure 2c2 and c4). Interestingly, cumulative histograms can differ significantly from those measured at equilibrium (Figure 2c), demonstrating how single molecule $Mg^{2+}$-jumps make possible the identification of intermediates inaccessible in equilibrium experiments.

Population relaxation kinetics also depend on the FRET state immediately before the jump. In particular, heterogeneity in the folding kinetics of state III distinguishes two states with the same FRET value (III and III*, Figure 2d), revealing the presence of hidden degrees of freedom (DOF) in the folding landscape (Figure 2d). Only jump intervals longer than five seconds allow more P RNA molecules to reach their native conformation through the hidden DOF (population relaxation).

Remarkably, $Mg^{2+}$-jump experiments make it possible to map the location of the energy barrier that induces the long memory effect by monitoring the single molecule trajectories and identifying the interconnection between different FRET states. A schematic free energy landscape for the P RNA can be depicted to summarize these results (Figure 2d). At low [$Mg^{2+}$] only two states are populated (I and IV), and therefore the other states must be higher in energy. Increasing [$Mg^{2+}$] induces electrostatic relaxation, and stabilizes the other states (II, III, III* and IV), which become more populated. Barrier-crossing transitions between these states follow and, subsequently, slow population relaxation takes place through the hidden DOF. A downward jump initiates unfolding, with first electrostatic relaxation of the potential landscape followed by population relaxation. Pre-equilibrium measurements provide a better understanding of the early folding dynamics of individual RNAs.

## Small RNAs use cooperativity for tertiary contact folding

Although RNA and proteins share some folding features, they also present significant differences. RNAs can form stable secondary structures even in the absence of tertiary interactions. Proteins use cooperative interactions to stabilize unique tertiary structures among numerous partially unfolded structures [31]. Cooperativity results in a sudden folding response to a small change in ligand or co-factor concentration [31–34]. The extent of cooperativity in RNA folding remains unknown.

Cooperativity is measured using double mutant thermodynamic cycles (Figure 3c). Herschlag and co-workers have recently characterized such a cycle for the P4-P6 domain of the *T. Thermophila* group I intron using smFRET (Figure 3a) [35•]. SMS provides a new approach to study cooperativity in RNA folding because it enables distinction of short-lived intermediates from minor subpopulations under identical conditions. This is important because tertiary contact ablations and mutations often result in large shifts in Mg-dependent folding, which may involve different (un)folded states.

P4-P6 consists of two side-by-side contacting RNA helices, connected by the J5/5a junction. Two major tertiary interactions stabilize the folded state: the metal-core/metal-core receptor (MC/MCR, Figure 3a, blue) and the tetraloop/tetraloop receptor (TL/TLR, Figure 3a, magenta). P4-P6 folds with high cooperativity with respect to [$Mg^{2+}$] and possible misfolded intermediates have been previously proposed [36]. The thermodynamic cycle for P4-P6 is shown in Figure 3c. To determine the equilibrium constants in the thermodynamic cycle the fluorophore labeled wild type (WT) and two ablation mutants were used (ΔMetal-core mutant, $I_{TL}$, and ΔTetraloop mutant, $I^{MC}$, Figure 3a). Figure 3b shows exemplary time trajectories and the corresponding

**Figure 2**

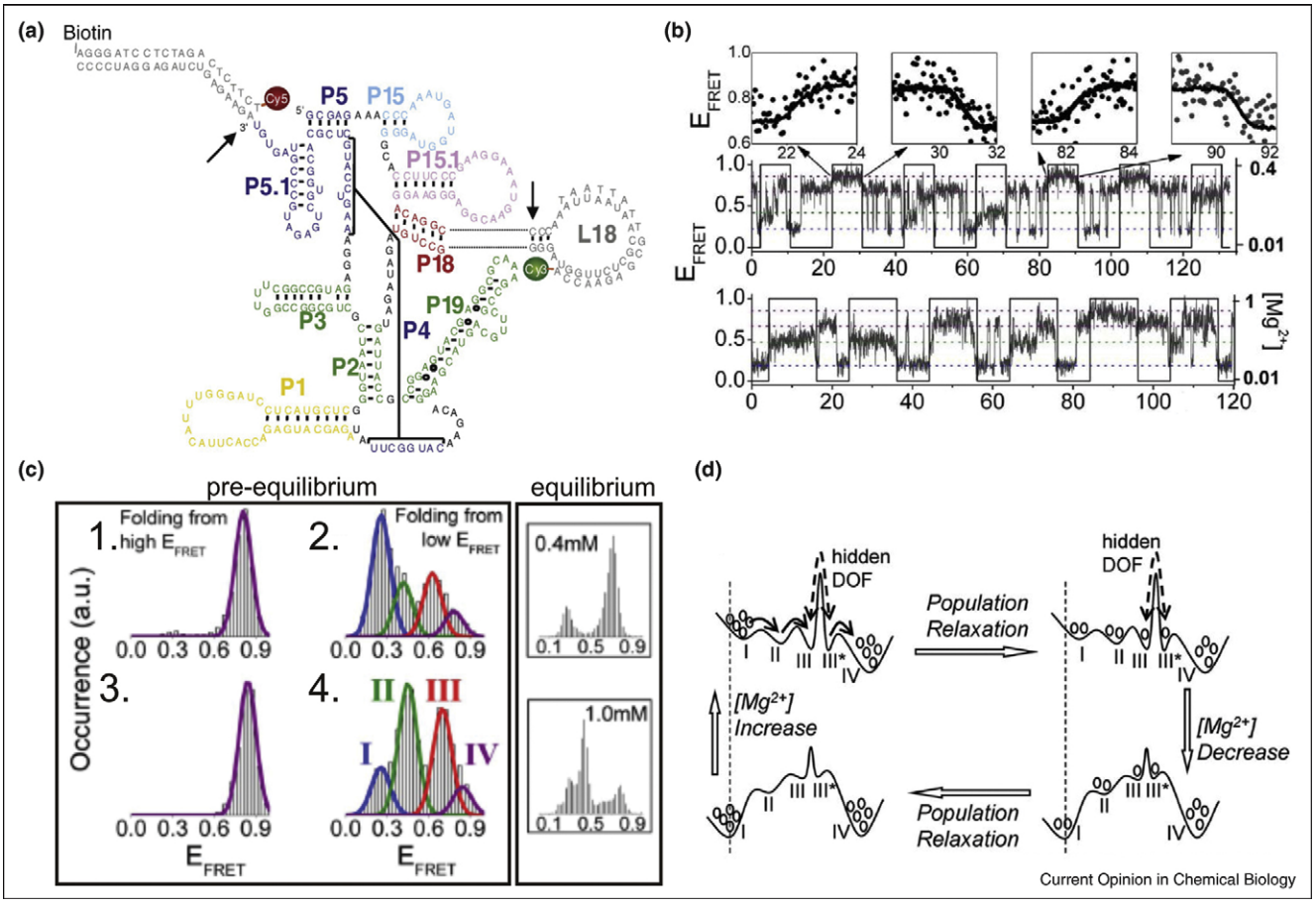


Modified secondary structure of RNase P RNA **(a)**, single molecule results from the pre-equilibrium $Mg^{2+}$-concentration effect study in the folding pathway of this large RNA **(b and c)**, and the free energy landscape of the folding pathways in presence and absence of $Mg^{2+}$ **(d)**. From reference [28•]. Reprinted with permission from PNAS.

histograms. All three constructs fluctuate randomly between two FRET levels: 0.1 (U state) and 0.8 ($I_{TL}$ or $F_{TL}^{MC}$) for the WT and the ΔMetal core complex, and 0.1 and 0.5 ($I^{MC}$) for the ΔTetraloop molecule. The equilibrium constants $K_{fold}$, $K_{MC}$, and $K_{TL}$ can be directly obtained from these histograms (Figure 3b). The WT spends most of its time in the folded state ($F_{TL}^{MC}$), while both mutants favor the unfolded state (U). Using the closed thermodynamic cycle properties, $K'_{MC}$ and $K'_{TL}$ can be readily calculated as $K'_{MC} = K_{fold}/K_{TL}$ and $K'_{TL} = K_{fold}/K_{MC}$. The tertiary contact cooperativity ($(\Delta G_{coop} = -RT\ln(K'_{TL}/K_{TL}) = -RT\ln(K'_{MC}/K_{MC}) = -3.2\,kcal/mol$) is 240-fold more favorable than the formation of both tertiary contacts cooperatively relative to their independent formation. This value is comparable to what is found in protein folding, but its physical origins are different. For example, cooperativity in RNA folding must involve electrostatic penalties for bringing negatively charged helices into close proximity. The presence of cooperativity in larger RNAs where tertiary contacts are farther away is an interesting issue that needs further exploration.

## Stepwise RNA folding during transcription

*In vitro*, RNA folding is typically triggered by addition of metal ions, but *in vivo*, the ionic strength of the cellular environment remains approximately constant during transcription. Understanding co-transcriptional folding is an important challenge to elucidate the structure–function relationship for RNA in living organisms. Block and co-workers have recently developed a new assay that mimics co-transcriptional folding using single molecule force spectroscopy [37,38••]. The idea consists of using a dual-trap optical tweezers configuration; on the first trap a dsDNA template (right, Figure 4b) is immobilized with a transcriptionally stalled single RNA polymerase (RNAP) molecule, while the initial RNA transcript emerging from RNAP is hybridized to the immobilized DNA handle on the second trap. This dumbbell geometry allows forces to be applied between the RNAP and the nascent RNA. An

**Figure 3**

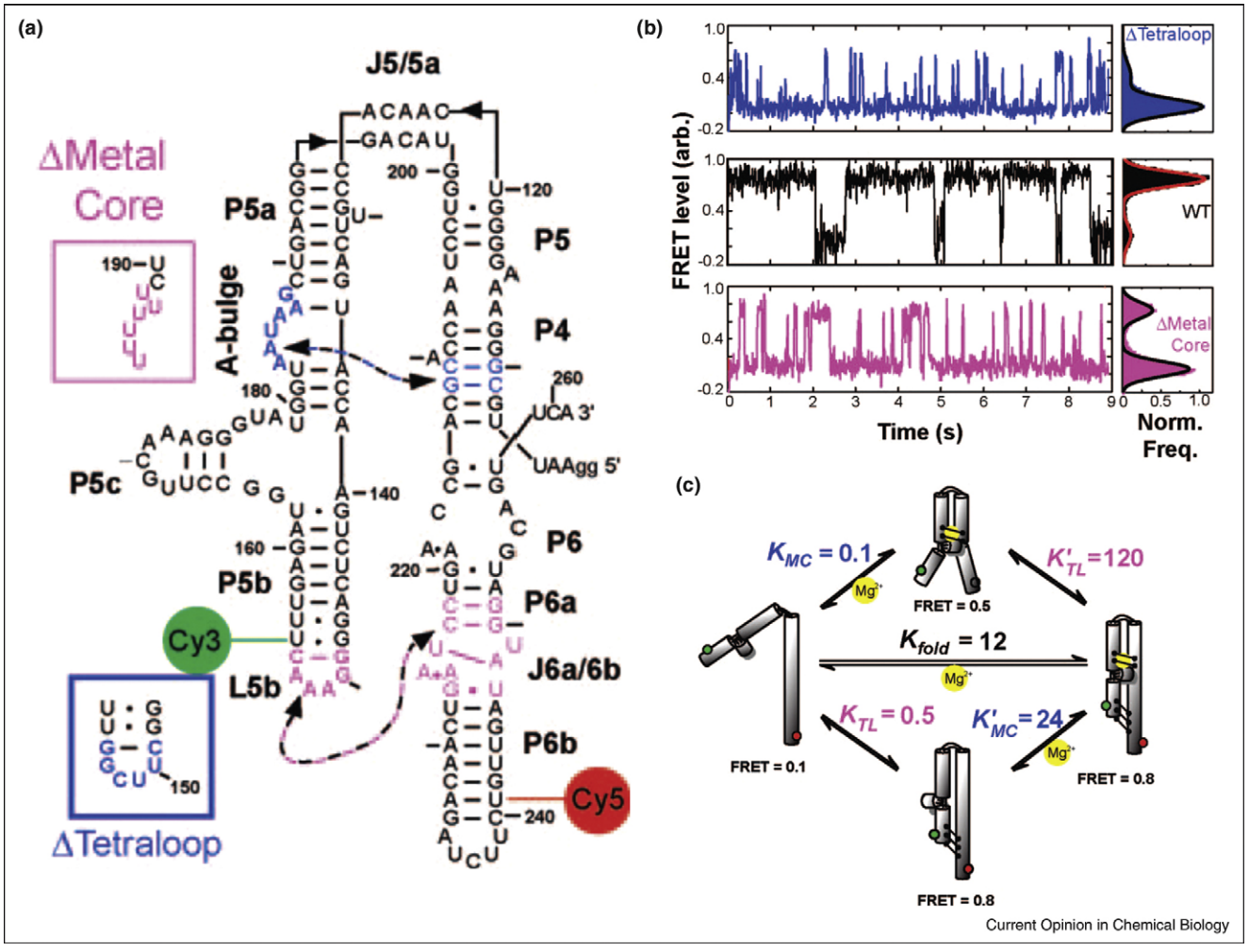


Single molecule results in the study of the cooperative tertiary contact in RNA folding. **(a)** Secondary structure of the P4-P6 domain of the *T. thermophila* group I intron. The P4-P6 molecule was labeled with a Cy3 donor (green) and Cy5 acceptor (red) for smFRET. **(b)** Single-molecule FRET trajectories. **(c)** Thermodynamic cycle to study folding cooperativity. The ensemble of unfolded conformations (U) comprises only secondary structure. U is in equilibrium with the native state ($F_{TL}^{MC}$, equilibrium constant $K_{fold}$). Two intermediates with one tertiary contact can form: $I^{MC}$ (only the MC receptor is active) and $I_{TL}$ (only the TL receptor is active), which can be formed from U with equilibrium constants $K_{MC}$ and $K_{TL}$, respectively, and then fold into $F_{TL}^{MC}$ with equilibrium constants $K'_{TL}$ and $K'_{MC}$, respectively. Reprinted with permission from reference [35•]. Copyright (2008) American Chemical Society.

adenine-binding riboswitch was used as a model system for this study. Riboswitches are found in the 5′-untranslated region (5′-UTR) of mRNA and control gene expression upon ligand binding [39,40].

Proper folding of riboswitches is important for gene regulation [38••,41]. The adenine riboswitch forms a three-helix junction (P1, P2, and P3, Figure 4a) [38••,39,41]. The folded state of the RNA is determined by using force-extension curves (FEC) in real time during aptamer transcription in the presence and absence of adenine (Figure 4a). In the absence of adenine, two unfolding events were identified and assigned to unfolding of P2 and P3, the most stable hairpins in the riboswitch (Figure 4c). In the presence of adenine, however, the FECs show that cooperative unfolding of the aptamer occurs occasionally through an intermediate state (Figure 4c). By correlating the extension of the molecule with the unfolding, the intermediate was identified as a collapsed complex with a pre-organized adenine binding pocket. The histograms in Figure 4e and 4f illustrate the observed states obtained from the complete trajectories in the presence and absence of adenine, respectively, at different forces.

Kinetic rates at 0 force can also be obtained by measuring FECs with different loading rates. Finally a co-transcriptional folding free energy landscape for the aptamer can

**Figure 4**

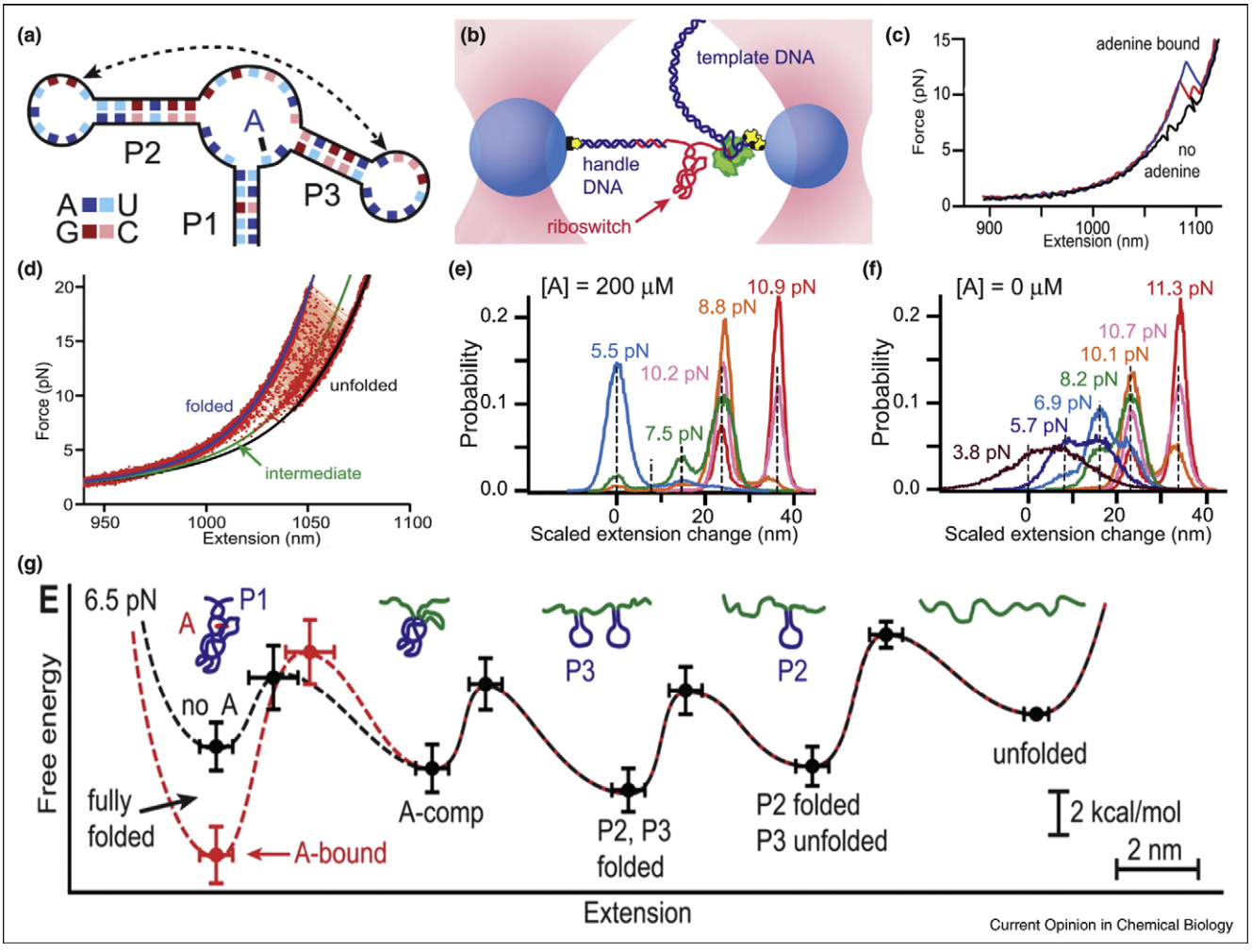


Co-transcriptional RNA folding study of a single riboswitch aptamer. **(a)** Aptamer secondary structure showing P1, P2 and P3 helices with their respective base pairing. **(b)** Dumbbell shaped optical trapping scheme, one bead is attached with a template dsDNA and other bead with cohesive DNA handle. This cohesive end of DNA handle is hybridized with RNA (red) transcribed by RNA polymerase (green). **(c)** Force-extension curves showing unfolding events of aptamer after RNA transcription. Black line with two events occurred in absence of adenine and blue line is in presence of adenine. In presence of adenine, an intermediate state is shown in red. **(d)** The distribution of unfolding forces showing three states folded, unfolded and intermediate. **(e)** Histogram showing trajectories at different forces scaled by the fractional extension per nucleotide at a given force. **(f)** Refolding histogram in absence of adenine showing the population of P1-unfolded and P1-folded states. **(g)** The energy landscape profile for stepwise refolding of aptamer showing five different folding states. Black line is in the absence of adenine and red line is in its presence. From reference [38••]. Reprinted with permission from AAAS.

be determined, in the presence and absence of the ligand (Figure 4g). This landscape suggests hierarchical folding including helical folding first followed by formation of the adenine binding pocket. Finally, adenine binding stabilizes the native state by $4 \pm 1$ kcal/mol (Figure 4g, red curve). These experiments highlight the importance of single molecule approaches in RNA co-transcriptional folding.

## RNA–protein complexes assemble hierarchically

Many essential RNAs require specific protein assistance to be functional *in vivo*. Protein–RNA interactions play an important role in the formation of these RNA–protein complexes (RNPs). SMS offers an interesting approach to study RNP biogenesis because it provides insight into the precise order in which folding intermediates are formed and their respective stabilities [42,43].

Recently, Zhuang and co-workers have characterized the assembly process of the *Tetrahymena* telomerase using smFRET [44••]. Telomerase is an RNP that helps to solve the end replication problem by adding DNA at the end of linear chromosomes [45,46]. The key components of the active complex are telomerase RNA and telomerase reverse transcriptase (TERT). A second protein, the

La-motif protein p65, binds the RNA specifically and stabilizes the RNP. Telomerase RNA has four stems (I through IV) and a large single stranded region that contains the template for DNA primer extension (Figure 5a).

To understand the assembly pathway of telomerase RNP, surface immobilized and fluorophore labeled telomerase RNA folding was monitored by smFRET in the presence and absence of p65 and TERT (Figure 5a). In the absence of protein, the single molecule FRET distribution is centered at 0.29 (Figure 5b, gray). Upon addition of p65 the FRET distribution shifts to 0.46 (Figure 5b, red) indicating the formation of a p65–RNA complex and a subsequent conformational change that brings the distal part of helix IV in close proximity to helix I (Figure 5a). Mutational data show that this helical bend occurs around the highly conserved GA bulge in stem IV. Addition of purified TERT to the p65–RNA complex yields a FRET distribution centered at 0.65 (Figure 5b, green), indicating the formation of the p65–RNA–TERT ternary complex. This structural change bends helix IV even closer to domain I.

Single molecule time trajectories allow monitoring of individual telomerase RNP in real time (Figure 5c). Addition of both p65 and TERT shows that the RNA–p65 complex forms first most of the time (red arrow), followed by binding of TERT (green arrow). The results

**Figure 5**

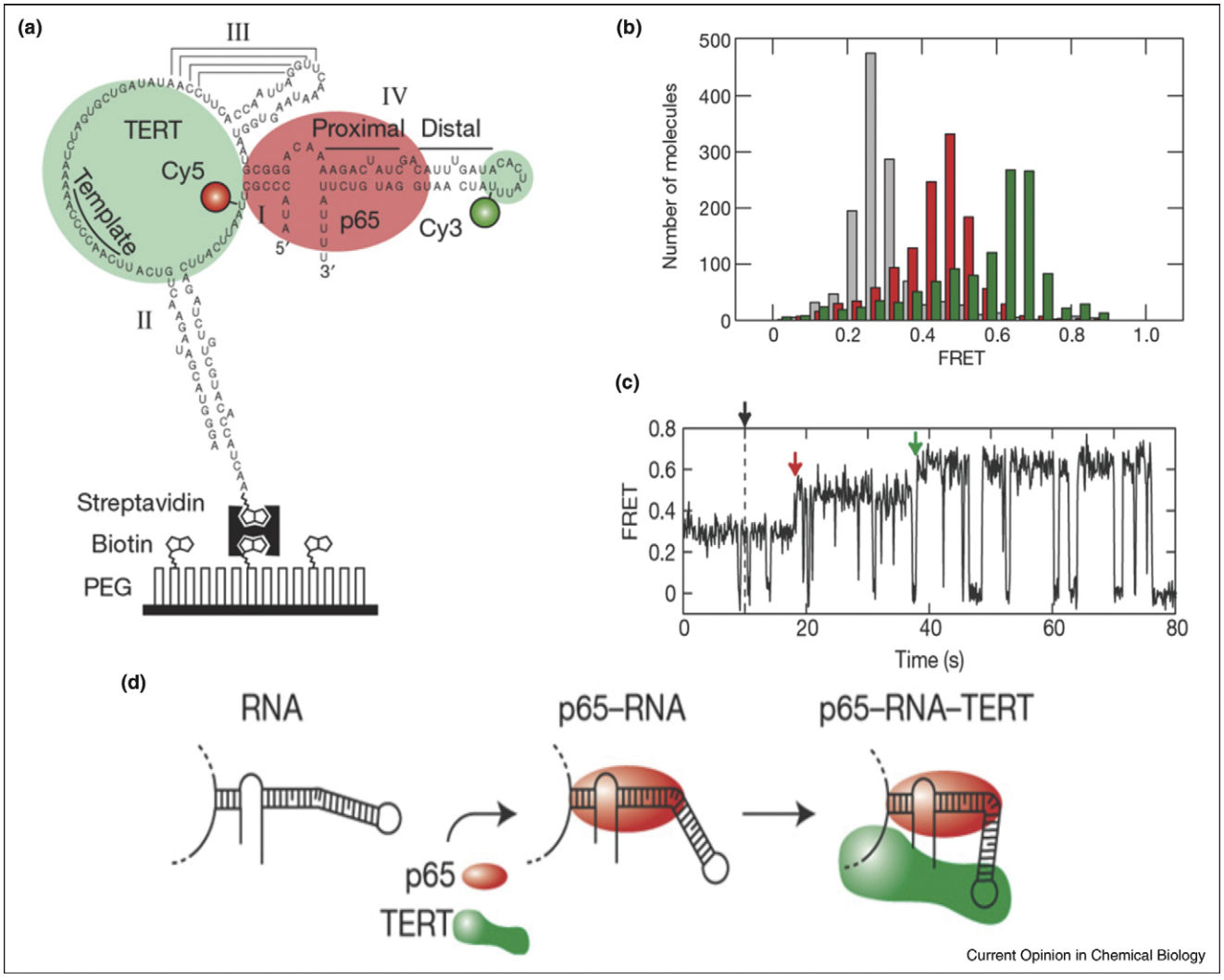


Protein assisted RNA folding in telomerase. **(a)** The Cy3 and Cy5 fluorophore labeled telomerase RNA is immobilized on a PEG coated glass slide via biotin and streptavidin interaction. Red and green circles are p65 and TERT interacting sites. **(b)** FRET histograms showing number of molecules at different FRET states, in absence of protein (gray), in presence of p65 only (red) and in presence of both p65 and TERT proteins (green). **(c)** FRET time trajectory showing folding of telomerase RNA in absence and presence of proteins p65 and TERT. Red arrow characterized the addition of p65 and green arrow is a mixture of p65 and TERT. **(d)** Schematic telomerase RNA folding where, p65 brings stem IV near to stem I in red followed by TERT binding in green. Adapted by permission from Macmillan Publishers Ltd: Reference [44••], copyright 2007.

indicate a hierarchical telomerase assembly process directed by sequential steps of protein-induced RNA folding (Figure 5d). However, minor alternative pathways are also possible (Figure 1). For example, TERT can first bind the RNA to form a less stable intermediate, and then p65 binds to form the final ternary complex. This work illustrates how single molecule approaches can elucidate RNP assembly pathways and uncover cooperative folding steps, such as the formation of the p65–RNA intermediate complex.

## Conclusions

Understanding how metal ions, proteins, and other cofactors induce RNA folding is essential to understanding and predicting RNA function *in vivo*. SMS offers new opportunities to study RNA folding from the nascent transcript to the native structure, because it readily enables monitoring and characterization of folding intermediates and transient conformations. Here, we have summarized recent developments that illustrate all of these aspects. Future developments in SMS will take the RNA folding problem from the test tube into the cell and will provide new insights into RNA folding *in vivo*.

## Acknowledgements

Financial support from Wayne State University (Start-up funds), the National Science Foundation (CAREER 0747285 to DR), and the NIH (GM085116) is gratefully acknowledged.

## References and recommended reading

Papers of particular interest, published within the period of review, have been highlighted as:

- • of special interest
- •• of outstanding interest


1. Hannon GJ, Rossi JJ: **Unlocking the potential of the human genome with RNA interference**. *Nature* 2004, **431**:371-378.
2. Mandal M, Boese B, Barrick JE, Winkler WC, Breaker RR: **Riboswitches control fundamental biochemical pathways in Bacillus subtilis and other bacteria**. *Cell* 2003, **113**:577-586.
3. Valadkhan S, Manley JL: **Splicing-related catalysis by protein-free snRNAs**. *Nature* 2001, **413**:701-707.
4. Gesterland R, Cech T, Atkins J: **The RNA World**. edn 2. Cold Spring Harbor, NY: Cold Spring Harbor Laboratory Press; 1999.
5. Khaled A, Guo S, Li F, Guo P: **Controllable self-assembly of nanoparticles for specific delivery of multiple therapeutic molecules to cancer cells using RNA nanotechnology**. *Nano Lett* 2005, **5**:1797-1808.
6. Novina CD, Sharp PA: **The RNAi revolution**. *Nature* 2004, **430**:161-164.
7. Rueda D, Walter NG: **Single molecule fluorescence control for nanotechnology**. *J Nanosci Nanotechnol* 2005, **5**:1990-2000.
8. Seetharaman S, Zivarts M, Sudarsan N, Breaker RR: **Immobilized RNA switches for the analysis of complex chemical and biological mixtures**. *Nat Biotechnol* 2001, **19**:336-341.
9. Sullenger BA, Gilboa E: **Emerging clinical applications of RNA**. *Nature* 2002, **418**:252-258.
10. •• Zhuang X, Kim H, Pereira MJ, Babcock HP, Walter NG, Chu S: **Correlating structural dynamics and function in single ribozyme molecules**. *Science* 2002, **296**:1473-1476.

Single molecule folding of the hairpin ribozyme shows evidence for folding heterogeneity and memory effects in folding.

11. •• Blanchard SC, Gonzalez RL, Kim HD, Chu S, Puglisi JD: **tRNA selection and kinetic proofreading in translation**. *Nat Struct Mol Biol* 2004, **11**:1008-1014.

This single molecule work monitors for the first time tRNA incorporation into the ribosome.

12. Hodak JH, Downey CD, Fiore JL, Pardi A, Nesbitt DJ: **Docking kinetics and equilibrium of a GAAA tetraloop-receptor motif probed by single-molecule FRET**. *Proc Natl Acad Sci U S A* 2005, **102**:10505-10510.
13. •• Bokinsky G, Rueda D, Misra VK, Rhodes MM, Gordus A, Babcock HP, Walter NG, Zhuang X: **Single-molecule transition-state analysis of RNA folding**. *Proc Natl Acad Sci U S A* 2003, **100**:9302-9307.

Characterization of the folding transition state of the hairpin ribozyme using single-molecule FRET.

14. • Liphardt J, Onoa B, Smith SB, Tinoco IJ, Bustamante C: **Reversible unfolding of single RNA molecules by mechanical force**. *Science* 2001, **292**:733-737.

Single-molecule RNA folding using force spectroscopy to investigate the unfolding mechanism of Tetrahymena ribozyme.

15. Xie Z, Srividya N, Sosnick TR, Pan T, Scherer NF: **Single-molecule studies highlight conformational heterogeneity in the early folding steps of a large ribozyme**. *Proc Natl Acad Sci U S A* 2004, **101**:534-539.
16. •• Zhuang X, Bartley LE, Babcock HP, Russell R, Ha T, Herschlag D, Chu S: **A single-molecule study of RNA catalysis and folding**. *Science* 2000, **288**:2048-2051.

Single-molecule RNA folding to study the folding and catalysis of the Tetrahymena group I intron ribozyme.

17. Bustamante C: **Unfolding single RNA molecules: bridging the gap between equilibrium and non-equilibrium statistical thermodynamics**. *Q Rev Biophys* 2006:1-11.
18. Weiss S: **Fluorescence spectroscopy of single biomolecules**. *Science* 1999, **283**:1676-1683.
19. • Rueda D, Bokinsky G, Rhodes MM, Rust MJ, Zhuang X, Walter NG: **Single-molecule enzymology of RNA: essential functional groups impact catalysis from a distance**. *Proc Natl Acad Sci U S A* 2004, **101**:10066-10071.

Single molecule FRET in combination with ensemble cleavage assays and kinetic simulations were used to reveal the presence of a network of coupled molecular motions connecting distant parts of the hairpin ribozyme.

20. Pyle AM: **Metal ions in the structure and function of RNA**. *J Biol Inorg Chem* 2002, **7**:679-690.
21. Takamoto K, Das R, He Q, Doniach S, Brenowitz M, Herschlag D, Chance MR: **Principles of RNA compaction: insights from the equilibrium folding pathway of the P4-P6 RNA domain in monovalent cations**. *J Mol Biol* 2004, **343**:1195-1206.
22. Treiber DK, Williamson JR: **Beyond kinetic traps in RNA folding**. *Curr Opin Struct Biol* 2001, **11**:309-314.
23. • Woodson SA: **Metal ions and RNA folding: a highly charged topic with a dynamic future**. *Curr Opin Chem Biol* 2005, **9**:104-109.

This review focuses on how ionic environments in contact with RNA molecules influence RNA folding.

24. • Bokinsky G, Zhuang X: **Single-molecule RNA folding**. *Acc Chem Res* 2005, **38**:566-573.

A very good review that describes previous studies in single-molecule RNA folding.

25. Onoa B, Tinoco I Jr: **RNA folding and unfolding**. *Curr Opin Struct Biol* 2004, **14**:374-379.
26. Zhuang X, Rief M: **Single-molecule folding**. *Curr Opin Struct Biol* 2003, **13**:88-97.
27. Draper DE, Grilley D, Soto AM: **Ions and RNA folding**. *Annu Rev Biophys Biomol Struct* 2005, **34**:221-243.
28. • Qu X, Smith GJ, Lee KT, Sosnick TR, Pan T, Scherer NF: **Single-molecule nonequilibrium periodic Mg2+-concentration jump**

**experiments reveal details of the early folding pathways of a large RNA**. *Proc Natl Acad Sci U S A* 2008, **105**:6602-6607.
Single-molecule FRET and [$Mg^{2+}$] jumps were used to study the pre-equilibrium RNA folding of the catalytic domain of Bacillus subtilis RNase P RNA.

29. Kurz JC, Fierke CA: **Ribonuclease P: a ribonucleoprotein enzyme**. *Curr Opin Chem Biol* 2000, **4**:553-558.

30. Rueda D, Hsieh J, Day-Storms JJ, Fierke CA, Walter NG: **The 5′ leader of precursor tRNA$^{Asp}$ bound to the Bacillus subtilis RNase P holoenzyme has an extended conformation**. *Biochemistry* 2005, **44**:16130-16139.

31. Ralston CY, He Q, Brenowitz M, Chance MR: **Stability and cooperativity of individual tertiary contacts in RNA revealed through chemical denaturation**. *Nat Struct Biol* 2000, **7**:371-374.

32. Baird NJ, Westhof E, Qin H, Pan T, Sosnick TR: **Structure of a folding intermediate reveals the interplay between core and peripheral elements in RNA folding**. *J Mol Biol* 2005, **352**:712-722.

33. Chauhan S, Woodson SA: **Tertiary interactions determine the accuracy of RNA folding**. *J Am Chem Soc* 2008, **130**:1296-1303.

34. Das R, Travers KJ, Bai Y, Herschlag D: **Determining the Mg2+ stoichiometry for folding an RNA metal ion core**. *J Am Chem Soc* 2005, **127**:8272-8273.

35. • Sattin BD, Zhao W, Travers K, Chu S, Herschlag D: **Direct measurement of tertiary contact cooperativity in RNA folding**. *J Am Chem Soc* 2008, **130**:6085-6087.
This study uses single-molecule FRET to characterize how tertiary interactions act cooperatively to drive RNA folding in the P4-P6 domain of *T. thermophila* group I intron ribozyme.

36. Deras ML, Brenowitz M, Ralston CY, Chance MR, Woodson SA: **Folding mechanism of the *Tetrahymena ribozyme* P4-P6 domain**. *Biochemistry* 2000, **39**:10975-10985.

37. Dalal RV, Larson MH, Neuman KC, Gelles J, Landick R, Block SM: **Pulling on the nascent RNA during transcription does not alter kinetics of elongation or ubiquitous pausing**. *Mol Cell* 2006, **23**:231-239.

38. •• Greenleaf WJ, Frieda KL, Foster DA, Woodside MT, Block SM: **Direct observation of hierarchical folding in single riboswitch aptamers**. *Science* 2008, **319**:630-633.
Here, dual-trap optical tweezers were used to study co-transcriptional folding of the aptamer domain of the adenine riboswitch at the single molecule level.

39. Lemay JF, Penedo JC, Tremblay R, Lilley DM, Lafontaine DA: **Folding of the adenine riboswitch**. *Chem Biol* 2006, **13**:857-868.

40. Coppins RL, Hall KB, Groisman EA: **The intricate world of riboswitches**. *Curr Opin Microbiol* 2007, **10**:176-181.

41. Winkler WC, Breaker RR: **Regulation of bacterial gene expression by riboswitches**. *Annu Rev Microbiol* 2005, **59**:487-517.

42. Bokinsky G, Nivon LG, Liu S, Chai G, Hong M, Weeks KM, Zhuang X: **Two distinct binding modes of a protein cofactor with its target RNA**. *J Mol Biol* 2006, **361**:771-784.

43. Ha T, Zhuang X, Kim HD, Orr JW, Williamson JR, Chu S: **Ligand-induced conformational changes observed in single RNA molecules**. *Proc Natl Acad Sci U S A* 1999, **96**:9077-9082.

44. •• Stone MD, Mihalusova M, O'Connor CM, Prathapam R, Collins K, Zhuang X: **Stepwise protein-mediated RNA folding directs assembly of telomerase ribonucleoprotein**. *Nature* 2007, **446**:458-461.
In this study, single-molecule FRET is used to reveal that the assembly of the telomerase RNP is a hierarchical process.

45. O'Connor CM, Collins K: **A novel RNA binding domain in tetrahymena telomerase p65 initiates hierarchical assembly of telomerase holoenzyme**. *Mol Cell Biol* 2006, **26**:2029-2036.

46. Collins K: **The biogenesis and regulation of telomerase holoenzymes**. *Nat Rev Mol Cell Biol* 2006, **7**:484-494.